International Journal of Multimedia and Ubiquitous Engineering
Vol.11, No.2 (2016), pp. 107-120
http://dx.doi.org/10.14257/ijmue.2016.11.2.13

4 Port Mobile Phone MIMO Antenna for the Femtocell Communications

Hyun-woong Hwang[1], Sun-Hyung Kim[2] and Taeho son[3]

Department of IT Engineering, Soonchunhyang University
[1]netwjstk@naver.com, [2]shkim@sch.ac.kr, [3]thson@sch.ac.kr

Abstract

In this paper, a 4-port broadband mobile phone multiple input multiple output (MIMO) antenna is designed and implemented for use in femto cell communications. The assembly consists of 4 antennas with one main antenna that covers the entire design band and 3 sub antennas that cover the data communication bands. Each of the antennas is located on the top and bottom corners of the bare board, and we tested them on a PC board with the same board ground circumstances as practical phone ground. The main antenna operates in the CDMA, GSM, LTE class 2~3 and class 33~34 service bands, and the sub antenna operates in the LTE class 1~4, and Wibro band for data communications. The voltage standing wave ratio (VSWR) was less than 3:1, and the maximum isolation between the antennas was -8.5dB over the entire design band. The average gains for the main antenna were measured from -2.48 to -0.54dBi, with efficiencies from 56.45 to 88.3% while those for the sub antennas were between -1.96 to -1.2dBi and 63.75 to 75.92%, respectively. The envelop correlation coefficient (ECC) for the MIMO system was under 0.148 over the entire data communications band.

Keywords*: Mobile antenna, MIMO, Femtocell, Hybrid antenna, ECC*

1. Introduction

Various studies that have focused on increasing communications bandwidth and improving signal quality for mobile communications are currently in progress. The 2G mobile communications have advanced to 3G and 4G technologies, research focusing on antennas for use in mobile phones is developing wider bandwidth with a greater multiple [1-3]. However, modern mobile phones, such as smartphones, have many limitations for the antenna design due to the wide ground area resulting from the large LCD screen and battery but a thin profile for the phone. This makes it difficult to improve bandwidth characteristics. Therefore many studies have proposed widening the bandwidth of the antenna [2-6]. To improve the bandwidth enhancement, the antenna can be inserted into small empty spaces in the phone [3], lumped elements can be applied at the antenna [4, 5], and the antenna can be implemented according to the ground of the phone [6].

One of the fundamental factors that can improve communications quality is to reinforce the base station. However, the interaction between base stations and the occurrence of shadow radio zones decreases the quality of the connectivity. This problem causes a decrease in the signal to noise ratio (SNR) of the receiver system, reducing the data speed [7]. Many studies have been conducted to solve this problem, and one of the technologies that had been studied the most involves using femtocell communications. The main purpose of femtocell communications is to reduce shadow radio zones. To this end, a large zone of an existing base station needs to be divided into many small femto zones. Femtocell communication systems are based on multiple input multiple output (MIMO) communications. MIMO communication systems select the signal that is most favorable among all signals affected by the fading in order to obtain diversity gain.

ISSN: 1975-0080 IJMUE

However, at least four antennas are required to obtain the optimum diversity gain under a femtocell environment. The reason for this is that it is difficult to obtain diversity gain since the difference between incoming signals is not large. Accordingly, several studies using 4 port antennas in the base station are in progress [8, 9]. However, research on the multi-port broadband MIMO antenna for use in mobile phones under femtocell communications still need to be performed.

In this paper, we design and implement a 4-port broadband mobile antenna for femtocell communications on a bare board of the same size as a practical mobile phone. Four antennas are used with one main antenna and 3 sub antennas. The main antenna operates over CDMA (824~896MHz) and GSM (880~960MHz) service bands (lower band), which carry voice communication bands, and LTE class 2 (1850~1990MHz), 3 (1710~1880MHz), 33 (1900~1920MHz), and 34 (2010~2025MHz) (upper band), which are the data communication bands. In addition, the 3 sub antennas resonate identically at the data communication bands and Wibro band (1710~2360MHz). The design for all antennas is based on the hybrid operation to obtain a wide bandwidth. The antennas are located at each of the corners on the top and bottom of the PC board. The structure of this paper involves checking the antenna parameters through a simulation in Section 2, "Antenna Design" and showing the measured data in Section 3, "Antenna implementation and measurement."

2. Antenna Design

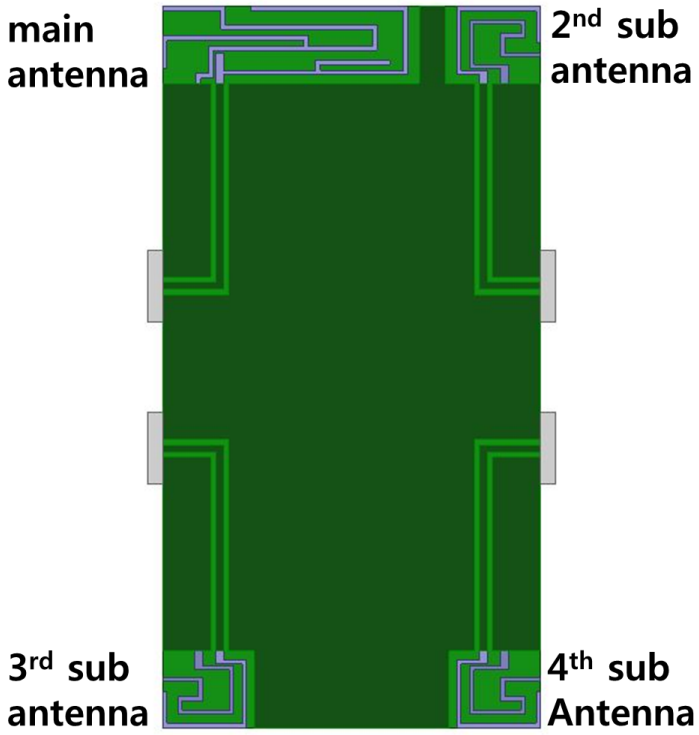

Figure 1. Figure of the Antenna Model

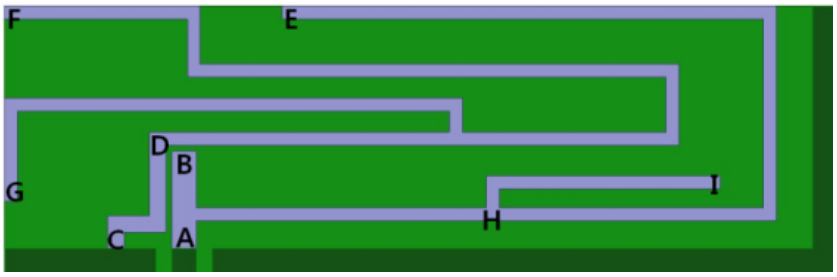

Figure 2. Main Antenna

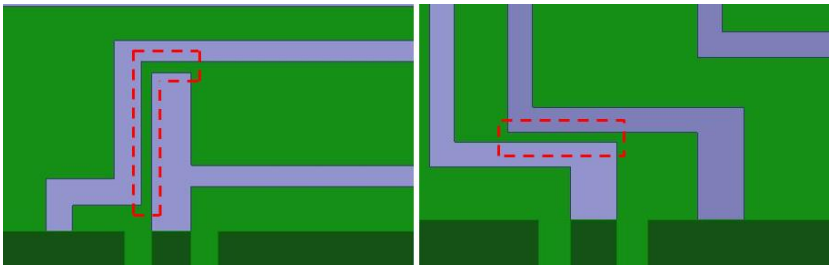

(a) Main Antenna (b) Sub Antenna

Figure 3. Coupling Structure of (a) Main and (b) Sub Antenna

Figure 1 shows the 4-port MIMO antenna model. The four antennas include a main antenna on the top left and 3 sub antennas at the other corners. It is designed in such a way that the ground between the antennas is the same as that of the environment of a practical mobile phone. The width and length of the PC board are 74.2 mm and 141.2 mm, respectively. An FR4 substrate of the relative dielectric constant ε_r= 4.4 with a thickness 0.8 mm is used. The design of all antennas is based on the monopole + inverted F antenna (IFA) hybrid antenna composed of a monopole antenna and an IFA fed by the coupling structure.

Figure 2 shows the pattern for the main antenna, and the main antenna has a width x length of 50.375 mm x 15mm.The antenna is designed in such a way that the monopole and the IFA are configured to conform to the resonance length of the quarter wavelength. The length of the main antenna is of 69.45 mm (A-E) for the monopole and 84.65 mm (D-F) for IFA. The length of the IFA stub and the monopole open stub are 53.6 mm (D-G) and 16.575 mm (H-I). The lengths of the monopole and the IFA provide resonances both at the lower band and the upper band while the lengths of the IFA stub and the open stub affect the upper band resonances. The width of the coupling conductor line (A-B) and (C-D) are of 1.5 mm and 1.0 mm, and the rest of the conductor line is of 0.8 mm.

Figure 3 shows the coupling structures as dot marks for the main antenna (a) and the sub antennas (b). The monopole antenna is fed from a coplanar waveguide with ground (CPWG) transmission line, and the IFA is fed from a monopole via the coupling structure. Therefore, a monopole and an IFA operate simultaneously through a hybrid form of operation. The hybrid dual resonances of the two antennas provide the antenna with wide bandwidth characteristics. The reason for which the width of the coupling conductor line is wider than that of the other conductors is that it is effectively coupled. The coupling space between monopole and the IFA is of 0.3 mm.

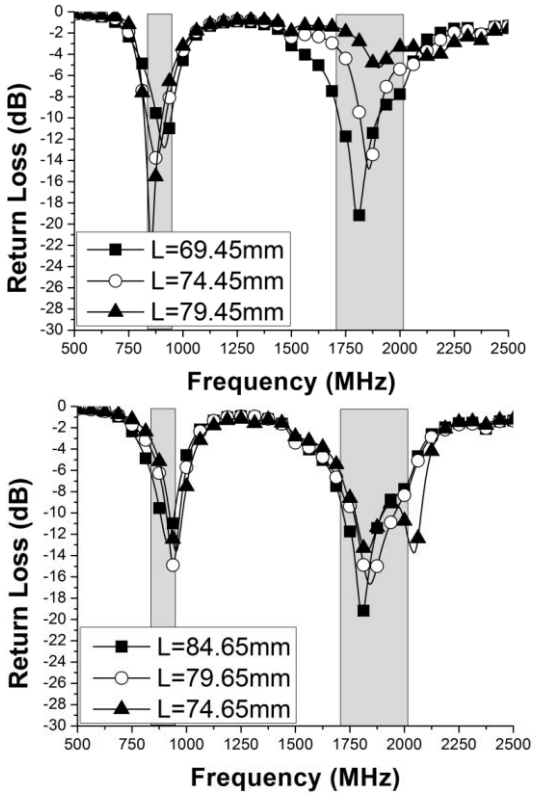

(a) Monopole Length (A-E) (b) IFA Length (D-F)

Figure 4. Variance of Return Losses as a Function of the Antenna Length (a) Monopole and (b) IFA

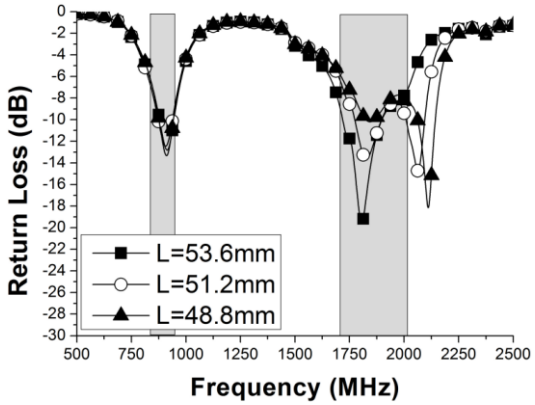

Figure 5. Variance of the Return Losses as a Function of the D-G Length

The resonances of the lower band are simulated as a functions of the length variances for the monopole line (A-E) and the IFA line (D-F) in Figure 4(a) and (b). For the simulation of characteristics of the antenna, Ansoft HFSS version 13 was used. In the monopole + IFA hybrid antenna, the lower band not only varies by the monopole but also the IFA. Therefore, the bandwidth for the given design can be achieved by adjusting the lengths.

When the length of the antenna is greater, the resonant frequency moves toward a lower frequency. Figure 4(a) shows that the length of the monopole antenna is seen to vary from 69.45 mm to 79.45 mm, in steps of 5 mm. When the length increases, the resonant frequency moves toward the lower frequencies. And in Figure 4(b), the length of the IFA varies from 78.64 mm to 88.65 mm, also in 5 mm steps.

The resonant frequency moves toward the same direction as that of the antenna of the monopole. The frequency multiplication in the lower band stub influences the upper band. Figure 5 shows that the length of the IFA stub line (D-G) affects the resonance of the upper band. The length of the stub changes from 48.8 mm to 53.6 mm, in steps of 2.4 mm. When the length of the stub is long, the resonant frequency of the upper band moves toward the lower direction.

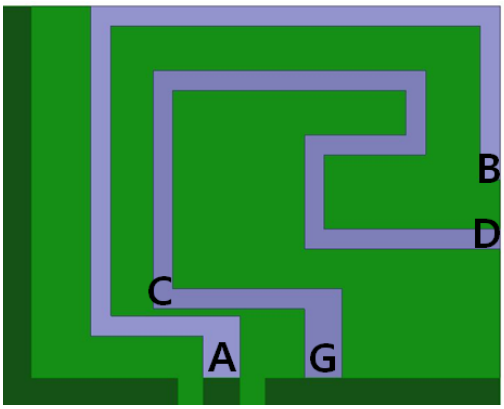

Figure 6. Sub Antenna

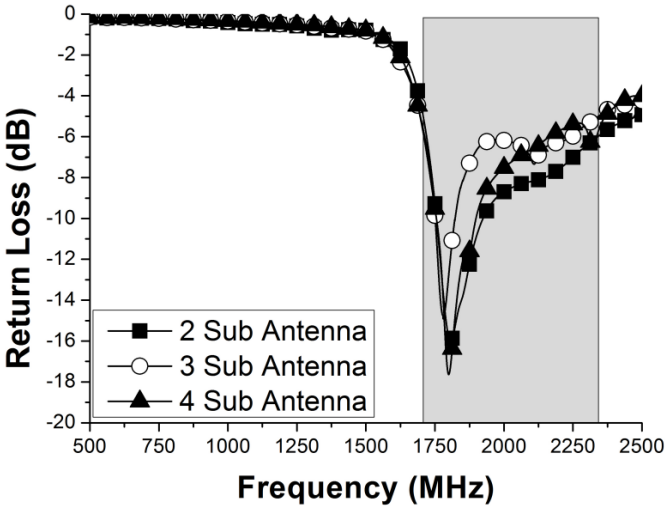

Figure 7. Return Losses of the Sub Antennas

Figure 6 shows the 3 sub antennas. The size of each sub antenna is 18.825 mm x 15 mm (width x length). The 3 sub antennas have the same dimensions and are also based on monopole + IFA hybrid operation. In Figure 6, the length of the monopole line (A-B), IFA line (C-D) and short stub of IFA (C-G) are 30.7 mm, 31.49 mm and 10.38 mm, respectively.

Figure 7 shows the simulated return losses for the 3 sub antennas. The resonance characteristics of each of the sub antennas in Figure 7 are basically same, but the impedances of each of the antennas are not the same. These are a result of the location of the sub antennas. The return losses for the 3rd and 4th sub antennas located at each side of the PC board, are the same.

However, return loss of the 2nd sub antenna that is just beside the main antenna, is not as same as return loss of 3rd sub antenna and 4th sub antenna. The influence of the coupling between the main antenna and the 2nd sub antenna are the cause of this

phenomenon. Nevertheless, the return losses of the 3 sub antennas are good as less than -6dB over the 1710 – 2360 MHz range of the data communication bands.

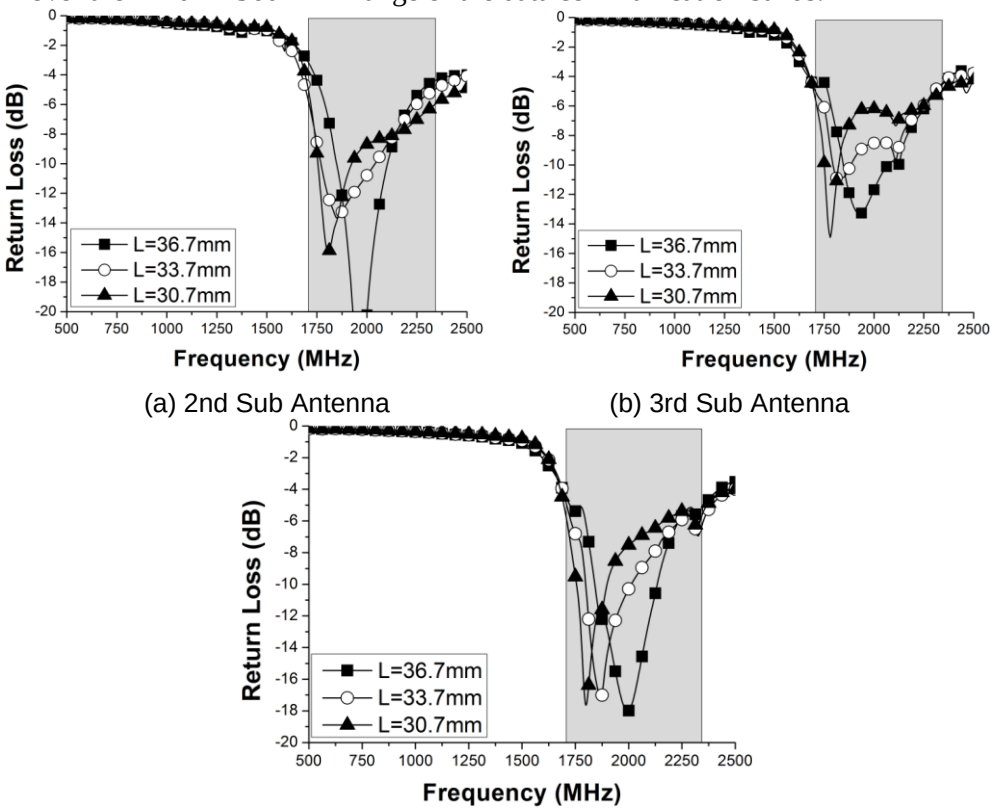

(a) 2nd Sub Antenna (b) 3rd Sub Antenna

(c) 4th Sub Antenna

Figure 8. Variance of Return Losses vs. Monopole Lengths (A-B) (A) 2nd Sub Antenna, (B) 3rd Sub Antenna, (C) 4th Sub Antenna

Table 1. The Optimized Dimensions of the Antenna

Description		Dimension(mm)
PC board Main antenna (in Figure 2)	PCB size	74.2 x 141.2
	space size	50.375 x 15.0
	A-E	69.45
	D-F	84.65
	D-G	53.6
	H-I	16.575
Sub antenna (in Figure 6)	space size	18.825 x 15.0
	A-B	30.7
	C-D	31.49
	C-G	10.38

The variances of the simulated return losses resulting from the monopole lengths (A-B) in Figure 8. The lengths of the monopole antenna line (A-B) change from 30.7 mm to 36.7 mm, in steps of 3 mm. When the lengths of the monopole are shorter, the resonant frequencies of (a) 2nd sub antenna, (b) 3rd sub antenna and (c) 4th sub antenna move toward higher frequencies, as shown in Figure 8. By the simulations as the function of lengths of the main and sub antenna, we have the final optimized dimensions for the proposed MIMO antenna as Table 1.

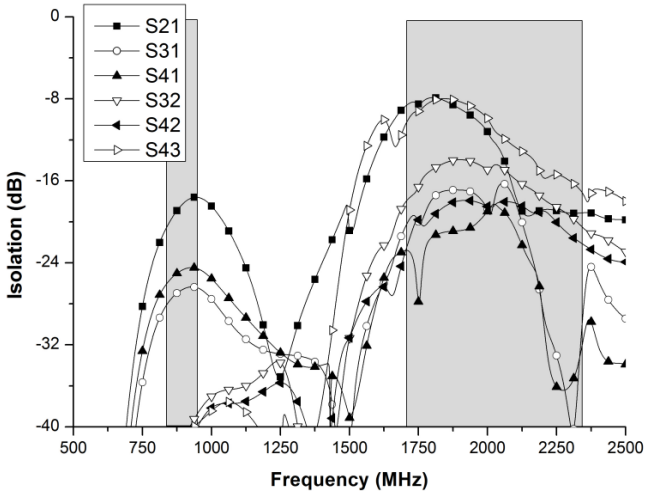

Figure 9. Simulated Isolations between 4 Antennas

Figure 9 shows the simulation of the isolation between the 4 antennas. The maximum isolation is simulated to be of -8.5dB over the entire design band, which is the specification of the maximum isolation at -8dB for the MIMO system.

3. Antenna Implementation and Measurement

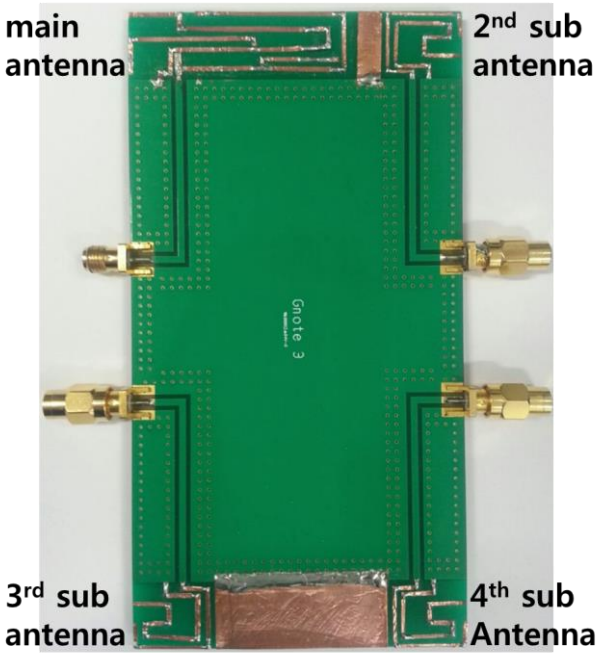

Figure 10. Implemented 4 Port Antenna

Figure 10 shows an implementation of the 4-port MIMO antenna, and the dimensions of the 4 antennas are as described in Section 2. The antenna is implemented on an FR4 PC board that a width and height of 74.2 mm and 141.2 mm. A copper tape is used for the antenna conductor line, which is the same as an implementation by an antenna engineer in a mobile phone company.

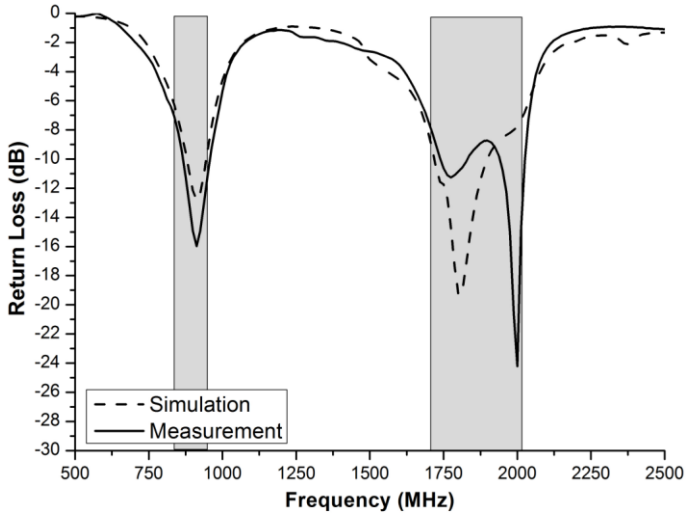

Figure 11. Return Losses of the Main Antenna

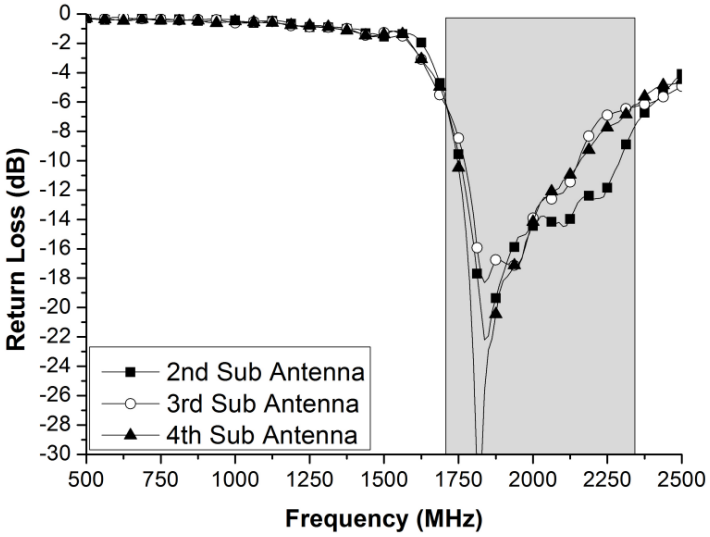

Figure 12. Measured Return Losses of the Sub Antenna

The return loss that was measured was compared to that obtained from the simulation shown in Figure 11. The return losses of the measurements and the simulation did not coincide exactly. This may be a result of an implementation error. The return losses at the beginning and at the end of the lower band and the upper band are -7.2 dB at 824MHz, -10.5 dB at 960MHz, –7.2 dB at 1710MHz and -11.2 dB at 2025MHz.

As shown in Figure 12, which measures the return losses of the sub antennas, all of the sub antennas satisfy a return loss of -6dB (within VSWR 3:1) on the 1710 ~ 2360MHz for the data communication bands. The return losses that were measured are in agreement with simulations in Figure 7.

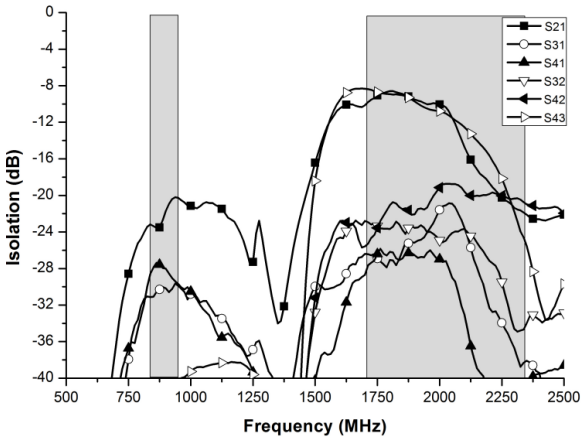

Figure 13. Measured Isolations between 4 Antennas

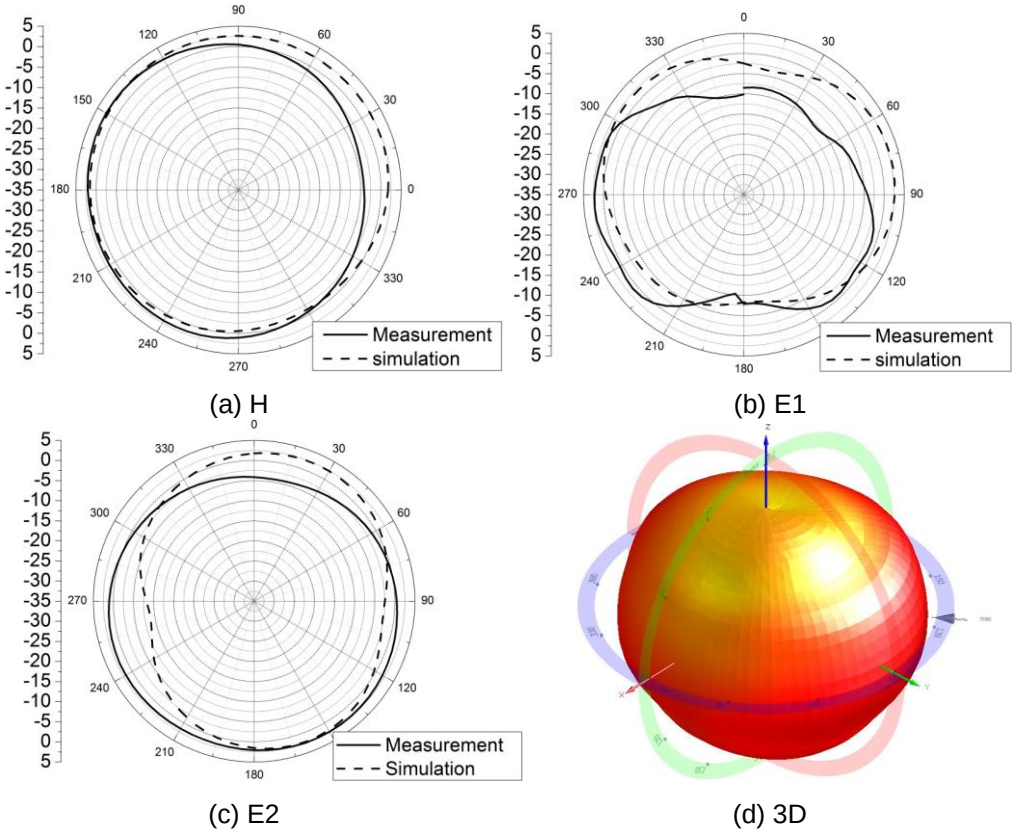

Figure 14. (a) H, (b) E1, (c) E2 Plane Radiation Patterns and (d) 3D Radiation Pattern for Main Antenna at 896MHz

Figure 13 shows the isolations that were measured between the 4 antennas, and the isolations satisfy a less than -8dB over the entire design band. The measured isolations are shown to have a slightly better isolation performance than those obtained through the simulations in Figure 9. These are also caused by an implementation error, but the trend for the isolations is identical.

A CSCM anti-reflective anechoic chamber made by MTG Co. in KOREA was used for the radiation measurements of the antenna that was implemented.

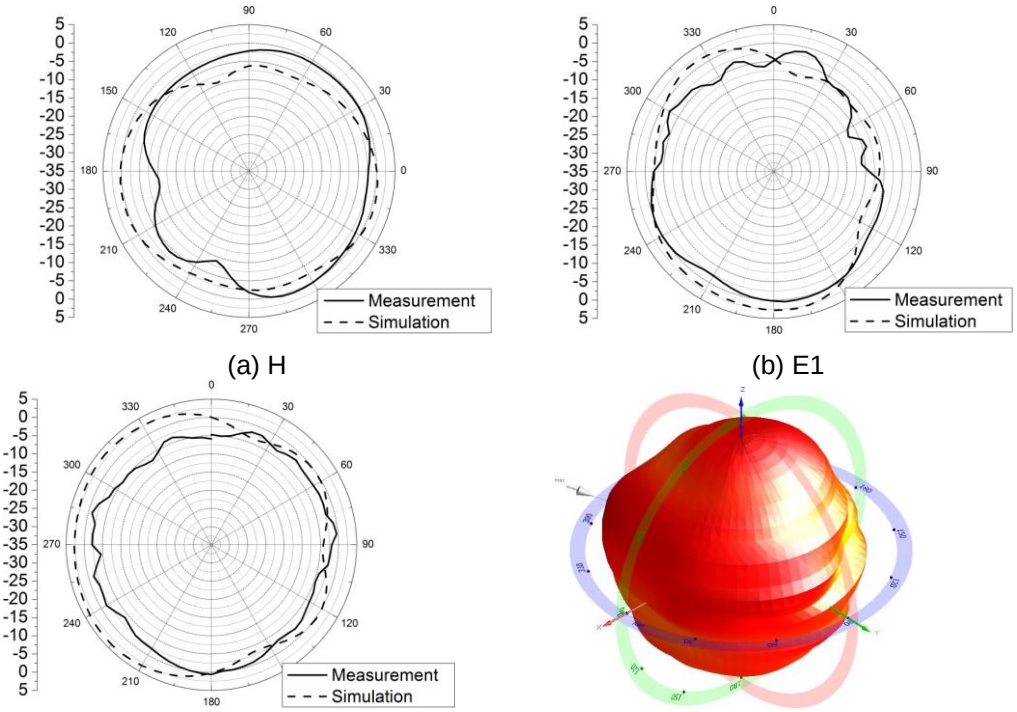

(a) H (b) E1

(c) E2 (d) 3D

Figure 15. (a) H, (b) E1, (c) E2 Plane Radiation Patterns and (d) 3D Radiation Pattern for Main Antenna at 1870MHz

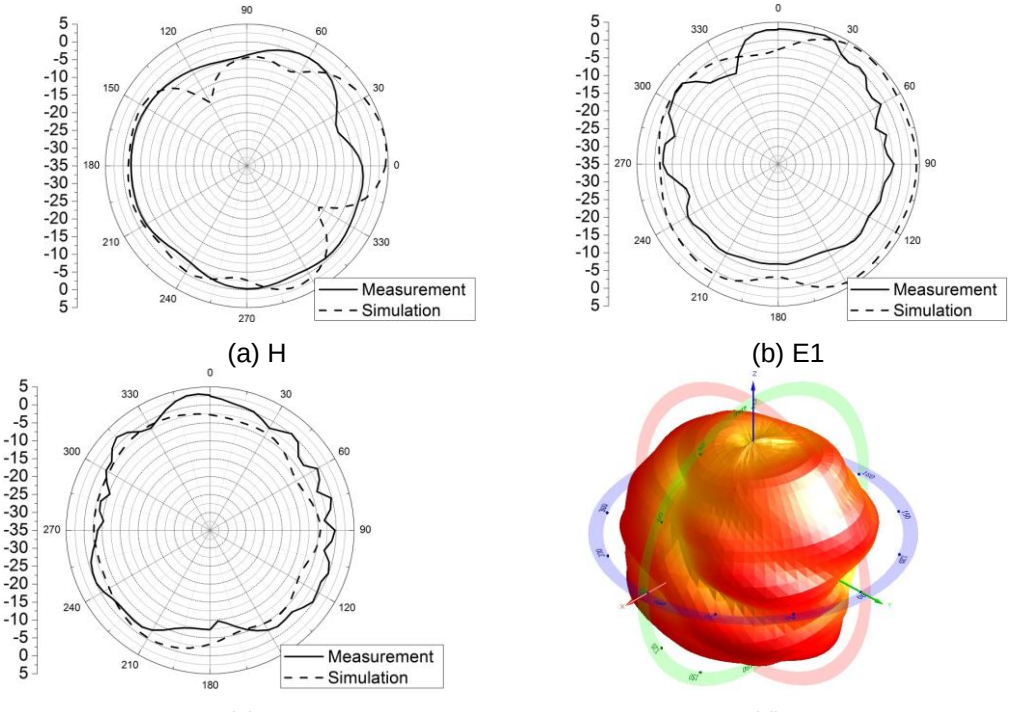

(a) H (b) E1

(c) E2 (d) 3D

Figure 16. (a) H, (b) E1, (c) E2 Plane Radiation Patters and (d) 3D Radiation Pattern for 2nd Sub Antenna at 1870MHz

Table 2. Average Gain vs. Field Planes for Sub Antenna

	2nd antenna	3rd antenna	4th antenna
H plane	-2.10	-1.28	-1.71
E1 plane	-2.13	-2.95	-2.97
E2 plane	-1.33	-0.06	-0.80

Table 3. Efficiencies and Average Gain of Main Antenna

Freq.[MHz]	Eff.[%]	Avg.[dBi]	Freq.[MHz]	Eff.[%]	Avg.[dBi]
824	56.45	-2.48	1710	57.96	-2.37
840	60.79	-2.16	1742	52.89	-2.77
861	67.88	-1.68	1790	57.77	-2.38
875	79.59	-0.99	1822	55.32	-2.57
889	82.35	-0.84	1854	55.69	-2.54
903	88	-0.56	1886	57.61	-2.24
919	88.3	-0.54	1918	56.34	-2.49
935	83.96	-0.76	1950	60.26	-2.2
951	81.82	-0.87	1992	70.19	-1.54
960	75.95	-1.19	2025	63.23	-1.99

In the chamber, the radiation patterns and efficiencies were measured against the frequencies for each port. Figure 14 shows two-dimensional 2D and 3D radiation patterns of the main antenna at 896MHz for the lower band. The H plane pattern is the fundamental pattern for the mobile phone and should be an omni-directional pattern without any nulls. The E1 and E2 plane patterns are the E plane patterns. The E1 plane is a front-back plane, and the E2 plane is a left-right plane for the mobile phone. The E1 plane pattern and the E2 plane pattern are not symmetrical for the mobile phone. The average gain measured for the H plane pattern at 896MHz is 0.44 dBi, as shown in Figure 14(a). The average gains of the E1 and E2 planes are -2.34dBi and -1.63dBi, as shown in Figure 14(b) and (c). The 3D radiation pattern is almost shown in the isotropic radiation in Figure 14(d). The 2D and 3D radiation patterns at a higher band of 1870MHz are shown in Figure 15(a), (b), (c) and (d). The average gains for the H, E1 and E2 planes were measured as -2.4dBi, -2.67dBi, and -2.49dBi, respectively. The H plane and the 3D patterns are in a slightly distorted shape when compared to that of the lower band, but are almost omni-directional with isotropy. Figure 16 shows 2D and 3D radiation patterns for the 2nd sub antenna. Because of the similarity the sub antenna's radiation pattern, 2D and 3D radiation patterns of 2nd sub antenna is representatively shown. The average gains are noted in the Table 2. The 3D radiation patterns of the sub antennas are shown to have all radiations based on the direction opposite to ground.

The radiation efficiency of an antenna is one of its important characteristics for us in mobile applications. The environment inside of the mobile phone, such as the presence of various components and small available space, affect the degradation in the characteristics, including the return loss, isolation and radiation. The antenna gain is related to the radiation efficiency. High radiation efficiency for the antenna is necessary for mobile communications.

Table 3 shows measurements for the efficiencies and the average gains of the main antenna. The efficiencies and the average gains of the main antenna are 56.45 ~ 88.3% and -2.48 ~ -0.54dBi, respectively.

Table 4. Efficiency and Average Gains of Sub Antennas

	2nd sub antenna		3rd sub antenna		4th sub antenna	
Freq.[MHz]	Eff.[%]	Avg.[dBi]	Eff.[%]	Avg.[dBi]	Eff.[%]	Avg.[dBi]

1710	72.2	-1.41	52.8	-2.77	58.92	-2.3
1772	73.22	-1.35	59.59	-2.25	64.29	-1.92
1866	67.18	-1.73	61.38	-2.12	64.47	-1.91
1928	75.57	-1.22	59.19	-1.6	71.09	-1.48
1990	75.92	-1.2	72.36	-1.41	73.37	-1.34
2052	70.33	-1.53	67.93	-1.68	67.12	-1.73
2114	67.69	-1.69	62.85	-2.02	60.95	-2.15
2176	67.71	-1.69	58.96	-2.29	58.69	-2.31
2280	63.75	-1.96	53.77	-2.69	54.24	-2.66
2360	68.08	-1.67	57.49	-2.4	58.02	-2.36

$$\rho_e = \frac{|S_{11}*S_{12}+S_{21}*S_{22}|^2}{(1-|S_{11}|^2-|S_{21}|^2)(1-|S_{22}|^2-|S_{12}|^2)} \quad (1)$$

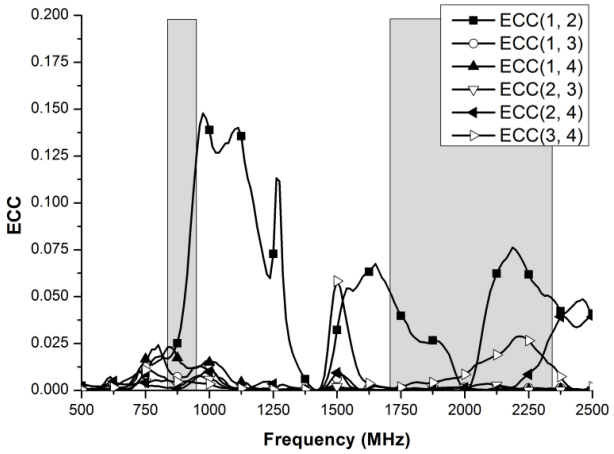

Figure 17. ECC from Measured Data

In Table 4, the efficiencies and the average gains for 3 sub antennas at the data communication band. The efficiencies of the sub antennas are 63.75 ~75.92%. The average gains are -1.96~ -1.2dBi for the sub antennas.

The envelope correlation coefficient (ECC) is very important for MIMO communication systems. ECC is related to the correlation between each of the antennas, and it affects to the SNR of the system. The formula to calculate the ECC calculation between the 2 antennas is presented as equation (1), which is a function of the S-parameters [10]. If the S21 and S12 isolations are smaller, ECC becomes lower and results in better performance for the MIMO communication system [11]. The S-parameters that were measured are used to calculate the ECC, as in Figure 17, with the maximum ECC between the 4 ports over the entire LTE data communication of 0.148. The channel capacity and channel correlation coefficient should be checked for the MIMO communications.

For the MIMO antenna, the isolation or the ECC between antennas are important parameters that are related to the channel capacity and channel correlation [12]. By the MIMO system specification of the mobile phone manufacturing companies in Korea, the isolation and ECC between the antennas are imposed below than -8dB and 0.2. Therefore, the proposed antenna can be applied as a MIMO antenna for femtocell mobile communications.

3. Conclusion

A 4-port mobile phone MIMO antenna that consists of one main antenna and 3 sub antennas was designed and implemented for femtocell communications. The design of all antennas is based on monopole + IFA hybrid operation. The 4 antennas were located at each of the corners of a board that had the same size as a practical mobile phone. The antenna was implemented on the bare board and was measured. The VSWR and the maximum isolation between the antennas were less than 3:1 and -8.5dB, respectively, over the entire design band. The 2D and 3D radiation pattern measurements revealed that the antenna radiated almost omni-directionally to the H plane and had isotropy in 3-dimensional space. The average gains and efficiencies that were measured were -3.44 ~ -0.7dBi and 45.29 ~ 85.08% for the main antenna and -3.44 ~ -2.35dBi and 51.3 ~ 71.72% for the 3 sub antennas. The maximum ECC from the S-parameters that were measured is 0.148 over the data communication bands. Therefore, this antenna can be applied as an antenna for mobile femtocell communications.

Acknowledgement

This research was supported by Basic Science Research Program Through the National Research Foundation of Korea (NRF) funded by the Ministry of Education (2015023260).

References

[1] X. Zhao, K. Kwon and J. Choi, "MIMO antenna using resonance of ground planes for 4G mobile application", The Journal of Korean Institute of Electromagnetic Engineering and Science, vol. 13, no. 1, **(2013)**, pp.51-53.
[2] S. Lim and T. Son, "Hybrid antenna for the all band mobile phone service including LTE", The Journal of Korean Institute of Electromagnetic Engineering and Science, vol. 22, no. 7, **(2011)**, pp.737-743.
[3] G. Yu, "Design of broadband antenna using the space of the mobile phone", M.S. thesis, Department of IT engineering, Soonchunhyang University, Korea, **(2014)**.
[4] G. Kim and B. Lee, "Metamaterial-based zeroth-order resonant antenna for MIMO applications", The Journal of Korean Institute of Electromagnetic Engineering and Science, vol. 13, no. 3, **(2013)**, pp. 195-197
[5] M. Hong and T. Son, "3 Dimensional mobile phone internal antenna using the helix element", The Journal of Korean Institute of Electromagnetic Engineering and Science, vol. 19, no. 9, **(2008)**, pp. 906-912.
[6] R. Zhang, Y. Liu, H. H. Kim and H. Kim, "Bandwidth enhancement of ground antenna using resonant feeding circuit", IET Electronics Letters, vol. 49, No. 7, **(2013)**, pp. 441-442.
[7] M. F. Tariq and A. Nix, "Area spectral efficiency of a channel adaptive cellular mobile radio system in a correlated shadowed environment", Proceedings of the 48th IEEE Vehicular Technology Conference, BS8 1UB, UK, May 18-21, **(1998)**.
[8] H. S. Kang, Y. I. Park, H. G Yong and B. S. Kim, "Design of SPA antenna using switch for 2.6GHz", The Journal of Korean Institute of Electromagnetic Engineering and Science, vol. 23, no. 10, **(2012)**, pp. 1137-1144.
[9] Jie-Bang Yan, J. T. Bernhard, "Design of a MIMO dielectric resonator antenna for LTE femtocell base stations", IEEE Trans. on Antennas and Propagation, vol. 60, no. 2, **(2012)**, pp.438-444.
[10] S. Blanch, J. Romeu and I. Corbella, "Exact representation of antenna system diversity performance from input parameter description", IET Electronics letters, vol. 39, no. 9, **(2003)**, pp.705-707.
[11] C. Votis, G. Tatsis and P. Kostarakis, "Envelope correlation parameter measurements in a MIMO antenna array configuration", Int'l J. of Communications, Network and System Science, vol. 3, no. 4, **(2010)**, pp. 350-354.
[12] M. U. Khan, W. A. A. Al-Saud and M. S. Sharawi, "Isolation Enhancement Effect on the Measured Channel Capacity of a Printed MIMO Antenna System", Proceedings of the 2014 8th IEEE Antennas and Propagation (EuCAP), 2014 8th European Conference, The Hague, April 6-11, **(2014)**.

Authors

Hyun-woong Hwang, Received his BS in IT engineering from Soonchunhayng University, Korea, in 2014. He is currently pursuing his MS in IT engineering at Soonchunhayng University, Korea. His current research interests include microwave circuit design and antennas.

Sun hyung Kim, received his B.S., M.S. and Ph.D. degrees in Electronic Engineering from Sungkyunkwan University, Korea, in 1979, 1981 and 1988, respectively. Since 1989, He has been a professor in Department of Information and Communication Engineering, Soonchunhyang University.

From 2005 to the Present, he was a vice-chairman of Korea University Invention Association. From 2013 to the present , he was a vice-chairman of Korea Institute Of Information Technology.

His research interests include Data Communication, Embedded system, Network, *etc.*

Taeho Son, received a B.S. degree, an M.S. degree, and a Ph.D. degree from Hanyang University, Korea, in 1979, 1986, and 1990, respectively. From 1981–1982, he was a researcher with the Radar Center at Ferranti Co., Edinburgh, Scotland. He worked for Gold Star Precision Company as a team leader of the Radar and RF system Division from 1978 to 1987. Since 1990, he has been a professor in the Department of IT Engineering at Soonchunhyang University, Korea. He was a chairperson at the Korea Institute of Intelligent Transportation System in 2011. Moreover, he was a technical advisor at several companies concerned with the RF system and mobile phones, and he is working for advanced antenna engineering at Skycross Korea Company, Korea. Currently, his research is mainly focused on the design of various antennas for mobile communication and electronic systems for vehicles.